University of Nebraska - Lincoln
DigitalCommons@University of Nebraska - Lincoln

Faculty Publications from Nebraska Center for Materials and Nanoscience

Materials and Nanoscience, Nebraska Center for (NCMN)

March 2004

Humidity effects on the determination of elastic properties by atomic force acoustic microscopy

D.C. Hurley
Materials Reliability Division, National Institute of Standards and Technology, Boulder, Colorado

Joseph A. Turner
University of Nebraska - Lincoln, jaturner@unl.edu

Follow this and additional works at: http://digitalcommons.unl.edu/cmrafacpub

Part of the Nanoscience and Nanotechnology Commons

Hurley, D.C. and Turner, Joseph A., "Humidity effects on the determination of elastic properties by atomic force acoustic microscopy" (2004). *Faculty Publications from Nebraska Center for Materials and Nanoscience*. 57.
http://digitalcommons.unl.edu/cmrafacpub/57

This Article is brought to you for free and open access by the Materials and Nanoscience, Nebraska Center for (NCMN) at DigitalCommons@University of Nebraska - Lincoln. It has been accepted for inclusion in Faculty Publications from Nebraska Center for Materials and Nanoscience by an authorized administrator of DigitalCommons@University of Nebraska - Lincoln.

HTML ABSTRACT + LINKS

JOURNAL OF APPLIED PHYSICS VOLUME 95, NUMBER 5 1 MARCH 2004

Humidity effects on the determination of elastic properties by atomic force acoustic microscopy

D. C. Hurley[a)]
Materials Reliability Division, National Institute of Standards and Technology, Boulder, Colorado 80305

J. A. Turner
Department of Engineering Mechanics, University of Nebraska, Lincoln, Nebraska 68588

(Received 21 October 2003; accepted 16 December 2003)

We have investigated how ambient humidity can affect quantitative measurements of elastic properties on the nanoscale. Using an emerging technique called atomic force acoustic microscopy (AFAM), two samples were examined: a thin film of fluorosilicate glass and a section of borosilicate glass. When experimental results were analyzed using a simple model of the atomic force microscope cantilever dynamics, values of the tip–sample contact stiffness k^* increased approximately linearly with relative humidity. The effect is believed to be due to the presence of a humidity-dependent layer of water on the sample. To account for this, the data analysis model was extended to include viscoelastic damping between the tip and the sample. A damping term proportional to the relative humidity was used. The revised values for k^* showed virtually no dependence on humidity. Thus, the subsequent calculations of the indentation modulus M from k^* yielded similar values regardless of measurement humidity. These results indicate that environmental conditions can influence quantitative nanoscale measurements of elastic properties, at least in some materials. © 2004 American Institute of Physics. [DOI: 10.1063/1.1646436]

I. INTRODUCTION

Atomic force acoustic microscopy (AFAM) is an emerging technique to determine elastic properties of thin films and surfaces. Based on atomic force microscope (AFM) techniques, AFAM can provide elastic property information with nanoscale spatial resolution. The feasibility of AFAM [and related methods such as ultrasonic atomic force microscopy and ultrasonic force microscopy (UFM)] to yield quantitative nanoscale information has been demonstrated by several authors.[1–4] In order for AFAM to realize its full potential, however, several issues related to quantitative measurements must be examined more thoroughly. Here, we present results to investigate one such issue, namely the effect of the relative humidity (RH) on quantitative AFAM measurements of elastic modulus. We show how RH effects can introduce a measurement artifact and how this can be overcome by including damping effects in the data analysis model.

II. EXPERIMENTAL METHODS

Figure 1 shows a schematic of our experimental AFAM apparatus. The principles of operation are described in more detail elsewhere.[2] The sample under investigation was bonded to a piezoelectric transducer placed on the AFM stage. The transducer was a commercially available ultrasonic longitudinal contact transducer. It was excited with a continuous sine wave using a computer-controlled function generator (frequency: 0.1–2.5 MHz; amplitude: 25–200 mV for our transducer). If the AFM cantilever was positioned close to, but not touching, the sample surface, the free-space flexural resonances of the cantilever were excited. The transducer excitation frequency was swept and the amplitude of the response of the cantilever at that frequency was detected by the AFM photodiode sensor using lock-in techniques. In this way, a spectrum of the vibration amplitude of the cantilever versus frequency was obtained. Next, the cantilever tip was lowered into contact with the sample and a second vibration amplitude spectrum obtained. From the two spectra, the frequencies of the lowest two flexural resonances of the cantilever, for both free-space and sample-coupled conditions, were determined using the process described below.

The AFM cantilever used in these experiments was a rectangular-shaped silicon cantilever approximately 230 μm long, 45 μm wide, and 8 μm thick. The nominal value of the cantilever spring constant k_c specified by the vendor was $k_c = 45.7$ N/m. We found that the two lowest free-space flexural vibrations of this cantilever occurred at $f_1^0 = 175.7 \pm 0.1$ kHz and $f_2^0 = 1134.4 \pm 0.1$ kHz. When in contact with the samples described below, the two lowest flexural resonances, f_1 and f_2, occurred in the range of 840–860 kHz and 1885–1930 kHz, respectively. The resonant frequencies were measured at three different cantilever static deflections $\delta = 15$, 25, and 40 nm. Given the vendor value of k_c, this corresponded to static applied forces F_N in the range of 0.7–1.8 μN.

The experimental values for the resonant frequencies were used to calculate the contact stiffness k^* between the tip and the sample. The procedure by which this was accomplished is described in more detail below. Spectra of the cantilever resonances were acquired not only when the tip was in contact with the test (unknown) sample, but also in contact with a reference material whose elastic properties

[a)]Electronic mail: hurley@boulder.nist.gov

Downloaded 29 Aug 2007 to 129.93.17.223. Redistribution subject to AIP license or copyright, see http://jap.aip.org/jap/copyright.jsp

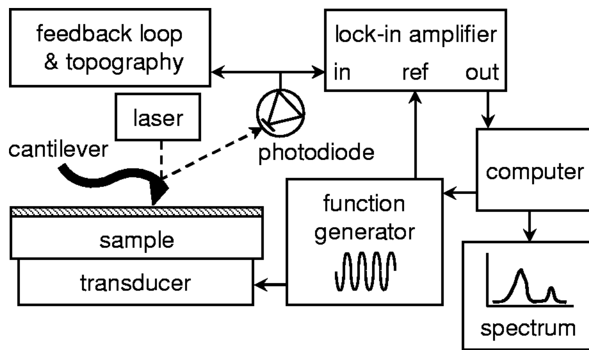

FIG. 1. Schematic of experimental AFAM apparatus.

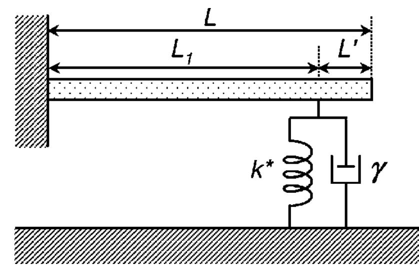

FIG. 2. Diagram of key features of AFAM model.

were known. The values of k^* for the test and reference samples were compared in order to obtain the desired quantity, the indentation or plane strain modulus M of the test sample. [For isotropic materials, $M=(E/1-\nu^2)$, where E is Young's modulus and ν is Poisson's ratio.] This approach eliminated the need to know parameters that are difficult to determine experimentally, such as tip radius.[5]

For the experiments described here, we monitored the RH during the AFAM measurements. Because our laboratory does not have humidity control, the values represent the ambient conditions at the time of the experiment. The RH meter contained a remote capacitive polymer sensor on a cable approximately 1 m long. The instrument accuracy specified by the vendor was $\pm 2\%$ and the resolution was 1%. Our AFM has an acoustic isolation hood that is placed over the apparatus during use. In these experiments, the samples were exposed to ambient conditions overnight. Each morning, the equipment was powered on and allowed to warm up for 2–3 h. The remote RH probe was placed close to the AFM head and the hood was closed while the measurements were made. Each set of measurements (that is, three different δ on one sample) typically took 15–20 min. The values indicated below are the average RH over this time. All of the measurements were made over the course of one week.

III. SAMPLE MATERIALS

AFAM experiments were performed on two samples. The test or unknown material was a thin film of fluorosilicate glass (FSG) on a (001) single-crystal silicon substrate. FSG, also known as fluorine-doped silicon oxide, is made by introducing fluorine during the deposition process of silica (SiO_2).[6] The resulting material contains a few atomic percent of flourine. (The exact processing conditions and composition of this particular film were not available.) FSG is of interest to the microelectronics industry as a replacement for SiO_2 in applications requiring a lower dielectric constant. The thickness of the film was measured by examining a sample cross section approximately 2 cm long in a field-emission scanning electron microscope (SEM). From six different SEM images of the cross section of the film, the average thickness d_{FSG} of the FSG film was found to be $d_{FSG}=3.08\pm 0.01$ μm.

A piece of Corning 7740 Pyrex borosilicate glass (Corning, Inc., Corning, New York),[7] approximately 0.5 mm thick, was used as the reference material in order to determine M_{FSG}, the indentation modulus of the FSG film. A value $M_{7740}=64\pm 2$ GPa of the indentation modulus M for the Pyrex 7740 sample was obtained by nanoindentation.[8] The value represents the average and standard deviation of 12 individual measurements.

IV. DATA ANALYSIS METHODS

To determine the tip–sample contact stiffness k^* from the cantilever resonant frequencies, we used a previously developed model.[9] When applied to a cantilever such as this one whose geometry closely approximates a rectangular beam of uniform cross section, the model has been shown to provide accurate modulus values for other materials.[2] The model describes the cantilever motion using conventional beam dynamics as depicted in Fig. 2. The cantilever is a beam of length L that is clamped at one end. The other end is free to vibrate (free-space condition) or else is coupled to the surface by a spring of stiffness k^* (sample-coupled condition). The spring is located at the position L_1 with respect to the clamped end of the cantilever. The remaining distance to the unclamped end is L'.

To include the effect of a viscoelastic interaction damping between the tip and the sample, a dashpot with characteristic damping γ in parallel with the spring is added. Closed-form analytical expressions can be written to characterize the beam dynamics of this system. Equations that relate the sample-coupled frequencies f_n to the contact stiffness k^* as a function of the relative tip position L_1/L have been developed previously for the case of no damping ($\gamma=0$).[9] In other work,[10] similar equations have been derived that include damping ($\gamma\neq 0$) but assume $L_1/L=1$. By combining these results, we obtain the following relation between f_n and k^* if both damping and tip position effects are considered:

$$\begin{aligned}
&\frac{2}{3}(k_nL_1)^3[1+\cos k_nL_1\cosh k_nL_1]\\
&\quad=\left(\frac{k^*}{k_c}+ip(k_nL_1)^2\right)[(1+\cos k_nL'\cosh k_nL')\\
&\qquad\times(\sinh k_nL_1\cos k_nL_1-\sin k_nL_1\cosh k_nL_1)\\
&\qquad+(1-\cos k_nL_1\cosh k_nL_1)(\sin k_nL'\cosh k_nL'\\
&\qquad-\cos k_nL'\sinh k_nL')],
\end{aligned}\tag{1}$$

where k_n is the wave number of the nth resonant mode. The damping constant p in Eq. (1) is given by

Downloaded 29 Aug 2007 to 129.93.17.223. Redistribution subject to AIP license or copyright, see http://jap.aip.org/jap/copyright.jsp

$$p = \frac{\gamma \omega_0}{k_c (k_1 L)^2}, \tag{2}$$

where $\omega_0 = 2\pi f_1^0$ is the angular frequency of the first free-space resonance and $k_1 L \approx 1.875$ is the first root of the free-space equation [Eq. (1) with $k^* = p = 0$]. Equation (1) was derived assuming that: (a) the tip experiences no lateral coupling and (b) the tip is perpendicular to the cantilever axis.

For a cantilever vibrating in free space, $k^* = p = 0$ and the right-hand side of Eq. (1) is zero. The roots $k_n^0 L$ of this modified equation can be found numerically. From the roots and the free-space frequencies f_n^0, one obtains the characteristic parameter $c_B L$ that contains the cantilever mass density, Young's modulus, and beam thickness:

$$c_B L = k_n^0 L / \sqrt{f_n^0}. \tag{3}$$

If damping effects are either not present or not accounted for when the cantilever is in contact with a sample ($p=0$), Eq. (1) and thus k_n is real. To find values for k^* from the resonant frequency spectra, $c_B L$ is first determined from f_n^0. Equation (3) is then used to determine the sample-coupled $k_n L$ from the sample-coupled f_n. Given the (real) values of $k_n L$, Eq. (1) is solved to determine k^* as a function of the effective tip position L_1/L for each flexural mode. The value of L_1/L for which both resonant modes yield the same value of k^* is considered to be the correct solution. We found that $L_1/L \approx 0.92$ for the cantilever used in these experiments.

If $p \neq 0$, that is, if damping effects are included, Eq. (1) and hence the k_n are complex. In this case, we again started by determining $c_B L$ from the free-space resonances using Eq. (3). Next, a value for the damping constant p was assumed. The root finder of a commercial software package was used to determine the complex values of $k_n L$ that satisfied Eq. (1). As an initial guess value for $k_n L$, we used the value calculated with Eq. (3) for $p=0$. From the roots, the real part of Eq. (1) was evaluated to find k^*. The calculated values of k^* for each mode were plotted as a function L_1/L. As before, the value of k^* and L_1/L, where the two modes intersected was taken as the solution.

The reduced modulus E^* and the indentation modulus M for the test material are determined from k^* and knowledge of the properties of the reference material:[5]

$$E^*_{\text{test}} = E^*_{\text{ref}} \left(\frac{k^*_{\text{test}}}{k^*_{\text{ref}}} \right)^n, \tag{4}$$

$$\frac{1}{E^*_{\text{test}}} = \frac{1}{M_{\text{tip}}} + \frac{1}{M_{\text{test}}}. \tag{5}$$

Here, the subscripts "test" and "ref" denote the properties of the test and reference materials, respectively. The value of the exponent n in Eq. (4) depends on the contact geometry. For Hertzian contact, $n=3/2$; for a flat-punch (flat) contact, $n=1$. Below, we cite values calculated with Eqs. (4) and (5) for $n=1$ only.

In these experiments, measurements of the contact stiffness k^*_{ref} for the Pyrex 7740 glass sample were first made at three different static deflections. Next, three measurements of k^*_{test}—that is, k^*_{FSG} for the FSG film—were made. Next, three additional measurements of k^*_{ref} were made. Individual

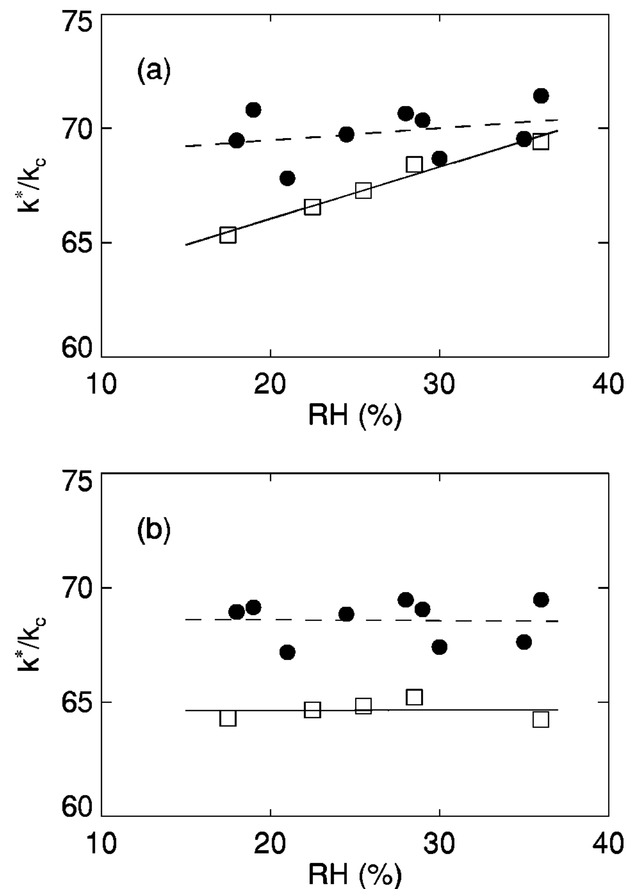

FIG. 3. Measured AFAM values of the normalized contact stiffness k^*/k_c vs RH for the fluorinated silica glass film (squares) and Pyrex 7740 glass samples (circles). The values in (a) were calculated with damping effects omitted (damping constant $p=0$). The values in (b) were calculated using $p = p' \times \text{RH}$ (%) with $p'_{\text{FSG}} = 8.9 \times 10^{-2}$ (%RH)$^{-1}$ and $p'_{7740} = 5.7 \times 10^{-2}$ (%RH)$^{-1}$. Lines indicate least-squares fits to the data points.

values of E^*_{test} were obtained from k^*_{ref} and k^*_{test} according to Eq. (4). Finally, the separate values of E^*_{test} were averaged and used to calculate a single value of M_{test} from Eq. (5). It can be seen in Eq. (5) that knowledge of the indentation modulus M_{tip} of the AFM cantilever tip is also needed. We used $M_{\text{tip}} = 161$ GPa corresponding to the value of M for the ⟨001⟩ silicon tip.

V. RESULTS AND DISCUSSION

Figure 3 shows our experimental results for the normalized contact stiffness k^*/k_c as a function of relative humidity RH for the FSG film and Pyrex 7740 glass samples. Figure 3(a) shows the calculated values with the damping constant $p=0$, that is, if damping effects are not included. Each point is the average of three separate values corresponding to the measurements at three different values of the static deflection δ. The measurement uncertainty in k^*/k_c due to data scatter and repeatability was approximately $\pm 2\%$. Figure 3(a) reveals that for both materials, k^*/k_c increased approximately linearly with RH. The effect was quite small for the 7740 glass sample (~1% over the RH range involved) and may not be significant given the measurement uncertainty. The

Downloaded 29 Aug 2007 to 129.93.17.223. Redistribution subject to AIP license or copyright, see http://jap.aip.org/jap/copyright.jsp

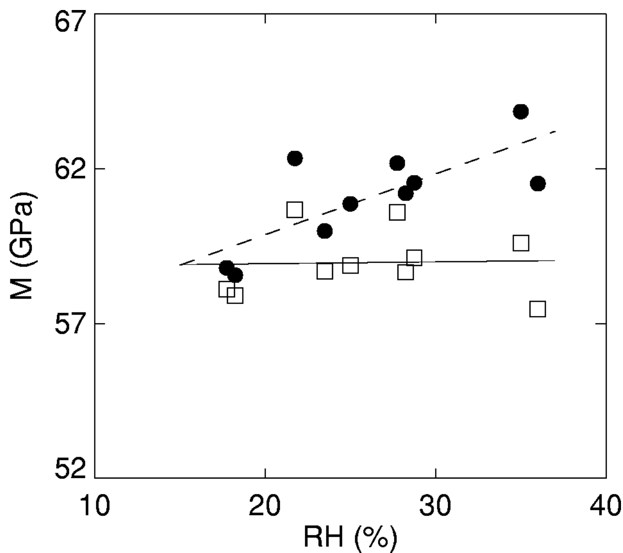

FIG. 4. AFAM values for the indentation modulus M_{FSG} vs RH. The circles indicate the values calculated from k^*/k_c in Fig. 3(a) for which damping effects are omitted (damping constant $p=0$). The squares represent the values obtained from k^*/k_c in Fig. 3(b) for which damping effects are considered. Lines show least-squares fits to the data.

effect was much more pronounced for the FSG film: k^*/k_c increased by $\sim$6% as the RH increased from 17.5% to 36%.

To include damping effects, we assumed that the damping constant p was proportional to the relative humidity:

$$p = p' \times \mathrm{RH}(\%). \tag{6}$$

The value of the proportionality factor p' was the same for all measurements on a given material but varied from material to material. For the FSG film, we used $p'_{FSG} = 8.9\times10^{-2}(\%\ \mathrm{RH})^{-1}$ [$\gamma_{FSG}=4.3\times10^{-6}$ N s/m in Eq. (2)]. For the Pyrex 7740 glass, $p'_{7740}=5.7\times10^{-2}(\%\ \mathrm{RH})^{-1}$ [$\gamma_{7740}=2.7\times10^{-6}$ N s/m in Eq. (2)].

The results for the normalized contact stiffness k^*/k_c from this calculation are shown in Fig. 3(b). It can be seen that by including a damping term in the data analysis, the apparent dependence of k^*/k_c on RH has been removed. Note that the specific values of p' (or γ) were chosen somewhat arbitrarily and were not calculated from independent information (e.g., Q factor of the resonant peaks). The point we intend to illustrate in this article is how a damping term can account for RH effects, and not how the term is quantitatively determined *a priori*. The degree to which the RH effects are removed might be improved if the values of p' used in the calculation were adjusted by approximately 5%–10%.

Figure 4 reveals how humidity can impact our ability to determine quantitative elastic properties with AFAM. The solid circles in Fig. 4 correspond to values for the indentation modulus M of the FSG film calculated from the "uncorrected" values of k^*/k_c in Fig. 3 (that is, with damping constant $p=0$). Each point represents the average of three different measurements. Measurement repeatability (data scatter between individual points) was typically 1 GPa or less. One element of uncertainty in the values of M_{FSG} is the accuracy of the measured value of the M_{ref}, that is, the modulus M_{7740} of the Pyrex 7740 sample. We estimate this component of the uncertainty to be approximately ±2 GPa. The effect of the uncertainty is to systematically shift all of the values of M_{FSG} up or down and does not alter any qualitative trends.

Figure 4 shows that the uncorrected values for M_{FSG} increase approximately linearly with RH. If the linear trend is ignored, the average value of the measurements is $M_{FSG}(\mathrm{uncorr}) = 61$ GPa±2 GPa. In contrast, the open square symbols in Fig. 4 show the values of the modulus M_{FSG} calculated from the "corrected" values of k^*/k_c that contain damping effects (that is, calculated with $p\neq0$). The apparent humidity dependence has been virtually eliminated. The average of these results is $M_{FSG}(\mathrm{corr}) = 59\pm1$ GPa.

A possible physical explanation for the observed humidity dependence is the presence of a water layer on the sample surface. If the thickness of the water layer increases with RH, then the apparent contact radius a between the tip and the sample increases accordingly. Because the contact radius and the contact stiffness are directly related through $k^* = a/(2E^*)$, k^* is also expected to increase with increasing RH. This is the effect illustrated in Fig. 3(a). As a matter of interest, numerical values were calculated for the contact radii a_{7740} and a_{FSG} of the Pyrex 7740 and FSG film samples, respectively. The measured values of k^* were used, along with $E^*_{7740}=46.5$ GPa and $E^*_{FSG}=55$ GPa. We found that a_{7740} varied from approximately 33 to 35 nm over the RH range reported and increased with RH. a_{FSG} increased with RH from about 36 to 39 nm over the same RH range.

It should be noted that FSG films have been previously observed to interact with atmospheric moisture.[6] Water absorption alters the dielectric constant of FSG and affects the stability and reliability of the film. Therefore, this effect has important implications for the use of FSG films in microelectronic devices. Several authors have investigated the water absorption phenomenon in FSG and its dependence on film properties such as fluorine content.[11,12] Due to these absorption effects, the dependence of k^* with RH in FSG may be stronger than in other common materials. Nonetheless, our results illustrate one way that AFAM methods may be adapted to suit a diverse range of technologically interesting materials.

To our knowledge, the effect of humidity on acoustic AFM measurements has not been investigated in detail. Dinelli *et al.*[13] performed experiments using a related technique, UFM. The contact stiffness for silicon (Si) and sapphire samples were measured as a function of applied load with a relatively soft ($\sim$3 N/m), V-shaped silicon cantilever. UFM experiments were performed at two or three different RH values. For sapphire, stiffness were generally lower at lower humidity (20% versus 75%). For (001) Si, stiffnesses at 18% RH were markedly lower, but values at 30% and 55% RH were roughly similar and showed no clear dependence. Because these materials are about three to six times stiffer than our samples and the cantilever is more than 15 times softer than ours, it is likely that a different regime of contact mechanics applies.

Downloaded 29 Aug 2007 to 129.93.17.223. Redistribution subject to AIP license or copyright, see http://jap.aip.org/jap/copyright.jsp

VI. SUMMARY AND CONCLUSIONS

We have investigated the effect of humidity on quantitative AFAM measurements of elastic properties. A thin film of fluorosilicate glass and a piece of Pyrex 7740 borosilicate glass were examined. When the cantilever dynamics were analyzed assuming elastic effects only, calculated values of the contact stiffness k^* increased approximately linearly with relative humidity. The data analysis model was extended to account for viscoelastic damping between the tip and the sample. A damping term proportional to the relative humidity was included. The revised values for k^* showed virtually no dependence on humidity. Thus, the subsequent calculations of the indentation modulus M from the contact stiffnesses yielded similar values regardless of the measurement of humidity.

These results indicate that environmental conditions can influence quantitative AFAM measurements of nanoscale elastic properties, at least for some materials. We plan to implement RH control on our AFM apparatus in order to study the effect systematically. Experiments will be performed to determine if the effect remains linear over a wider range of RH. In addition, a variety of materials will be examined to investigate which types are most susceptible to this behavior. Such experiments may also reveal a way to determine quantitative values for p or a related parameter from the measurable quantities.

ACKNOWLEDGMENTS

The FSG sample was provided by G. Pharr and A. Rar (U. Tennessee and Oak Ridge National Laboratory). R. H. Geiss (NIST) performed the SEM measurements of the film thickness and T. P. Butler (U. Nebraska) made the instrumented indentation measurements on the Pyrex sample. The authors thank M. Kopycinska-Müller (IZFP, Germany) and P. S. Rice (NIST) for valuable technical discussions. One of the authors (J.A.T.) acknowledges the support of the National Science Foundation (Grant Nos. DMI-0210850 and INT-0089548) and the Department of Energy (Grant No. DE-FG02-01ER45890). The University of Nebraska Foundation is also gratefully acknowledged for supporting the purchase of the instrumented indentation facilities.

[1] U. Rabe, M. Kopycinska, S. Hirsekorn, J. M. Saldana, G. A. Schneider, and W. Arnold, J. Phys. D **35**, 2621 (2002).
[2] D. C. Hurley, K. Shen, N. M. Jennett, and J. A. Turner, J. Appl. Phys. **94**, 2347 (2003).
[3] T. Tsuji and K. Yamanaka, Nanotechnology **12**, 301 (2001).
[4] R. E. Geer, O. V. Kolosov, G. A. D. Briggs, and G. S. Shekhawat, J. Appl. Phys. **91**, 4549 (2002).
[5] U. Rabe, S. Amelio, M. Kopycinska, S. Hirsekorn, M. Kempf, M. Göken, and W. Arnold, Surf. Interface Anal. **33**, 65 (2002).
[6] M. G. Shapiro, S. V. Nguyen, T. Matsuda, and D. Dobuzinsky, Thin Solid Films **270**, 503 (1995).
[7] Material trade names are identified to foster understanding. Such identification does not imply recommendation or endorsement by the National Institute of Standards and Technology, nor does it imply that the materials or equipment identified are necessarily the best available for the purpose.
[8] W. C. Oliver and G. M. Pharr, J. Mater. Res. **7**, 1564 (1992).
[9] U. Rabe, S. Amelio, E. Kester, V. Scherer, S. Hirsekorn, and W. Arnold, Ultrasonics **38**, 430 (2000).
[10] U. Rabe, J. A. Turner, and W. Arnold, Appl. Phys. A: Mater. Sci. Process. **66**, S277 (1998).
[11] M. Yoshimaru, S. Koizumi, and K. Shimokawa, J. Vac. Sci. Technol. A **15**, 2915 (1997).
[12] S. P. Kim, S. K. Choi, Y. Park, and I. Chung, Appl. Phys. Lett. **79**, 185 (2001).
[13] F. Dinelli, S. K. Biswas, G. A. D. Briggs, and O. V. Kolosov, Phys. Rev. B **61**, 13995 (2000).

Downloaded 29 Aug 2007 to 129.93.17.223. Redistribution subject to AIP license or copyright, see http://jap.aip.org/jap/copyright.jsp